Cross-Linkable Molecular Glasses: Low Dielectric Constant Materials Patternable in Hydrofluoroethers

Eisuke Murotani,[†,‡] Jin-Kyun Lee,[†] Margarita Chatzichristidi,[†] Alexander A. Zakhidov,[†] Priscilla G. Taylor,[†] Evan L. Schwartz,[†] George G. Malliaras,[†] and Christopher K. Ober*[,†]

Department of Materials Science and Engineering, Cornell University, Ithaca, New York 14853, and Asahi Glass Company, Ltd., 1150 Hazawa-cho, Yokohama-shi, Kanagawa-ku, Kanagawa 221-8755, Japan

ABSTRACT We report a new approach to solution-processable low-dielectric-constant (low-*k*) materials including photolithographic patterning of these materials in chemically benign and environmentally friendly solvents. A series of semiperfluorinated molecular glasses with styrenic substituents were successfully synthesized. These small molecular materials were thermally stable up to 400 °C and also exhibited an amorphous nature, which is essential to forming uniform films. Differential scanning calorimetry studies revealed that a cross-linking reaction occurred in the presence of acid, resulting in the formation of robust polymeric films. Atomic force microscopy images of the cross-linked films showed uniform and pinhole-free surface properties. Dielectric constants determined by a capacitance measurement were 2.6−2.8 (100 kHz) at ambient conditions, which are comparable to other polymeric low-*k* materials. The incorporation of semiperfluorinated substituents was effective in decreasing the dielectric constant; in particular, the fluorinated alkyl ether structure proved best. In addition, the fluorinated substituents contributed to good solubility in hydrofluoroether (HFE) solvents, which enabled the successful photolithographic patterning of those materials in HFEs down to a submicrometer scale.

KEYWORDS: low dielectric constant • molecular glass • cross-linking • micropatterning • photolithography • hydrofluoroethers

INTRODUCTION

A trend in the microelectronics industry is to provide higher performance integrated circuits while decreasing their size. This approach necessitates the construction of circuits employing multiple layers of interconnects with minimum wire width and submicrometer spacing. However, the miniaturization of device components also generates problems including interconnect signal delay (RC delay), cross-talk noise, and power dissipation, which compromise the device performance. The RC delay and cross-talk noise are proportionally related to the resistance of the wiring metal and/or dielectric constant (*k*) of the insulating material between lines or layers (1). Hence, following the introduction of copper as a wiring material with 36% lower resistance than aluminum, the focus in reducing the RC delay and cross-talk noise has shifted to low-*k* insulators.

In order to reduce the dielectric constant of a material, various approaches have been extensively explored in the past decade (2−9). Because the *k* values of a material depend upon the density and polarizability, increasing the free volume inside the film and reducing the polarizable moieties are straightforward strategies for material design. Lowering density has been studied by introducing pores into the film or appending sterically bulky moieties into the molecular structure. While those porous films successfully provided dielectric constants of down to 1.8 (3, 4, 9), a loss of mechanical toughness due to the fragile pores during subsequent processing steps remains a significant problem. Materials involving bulky molecular structures seem promising for robust insulating layers, although they tend to be brittle (1, 5). In addition to these approaches, it has been identified that the incorporation of fluorinated substituents into a molecular framework effectively reduces *k* values because of the low atomic polarizability of the electronegative fluorine atom and low polarizability of the C−F bonds against externally applied electric fields as well as an increase in the free volume (1, 10). Several polymers with fluorinated cores or side chains have been studied for this application (11−16).

Polymeric low-*k* materials are attracting a great deal of attention because of their potential for solution processability and mechanical flexibility. A number of polymers have been proposed for this application, including polyimides, poly(aryl ether)s, polynorbornenes, benzocyclobutene resins, or poly(naphthylene)s, some of which have already found commercial applications. Although polymeric materials possess the inherent advantage of robust film formation and good electrical performance, they also have potential concerns for their insufficient solubility and/or relatively high viscosity for efficient processing. An ingenious alternative to relieve these issues is to employ more soluble, small molecular precursors that can be transformed into robust polymer films via cross-linking processes after deposition (17). Another accompanying benefit of this approach is that

* Corresponding author. Tel: 607-255-8417. Fax: 607-255-2365. E-mail: cko3@cornell.edu.

Received for review July 26, 2009 and accepted September 23, 2009

[†] Cornell University.

[‡] Asahi Glass Company, Ltd.

DOI: 10.1021/am9004978

© 2009 American Chemical Society

Scheme 1. Synthetic Routes for 3 and 6a−6d[a]

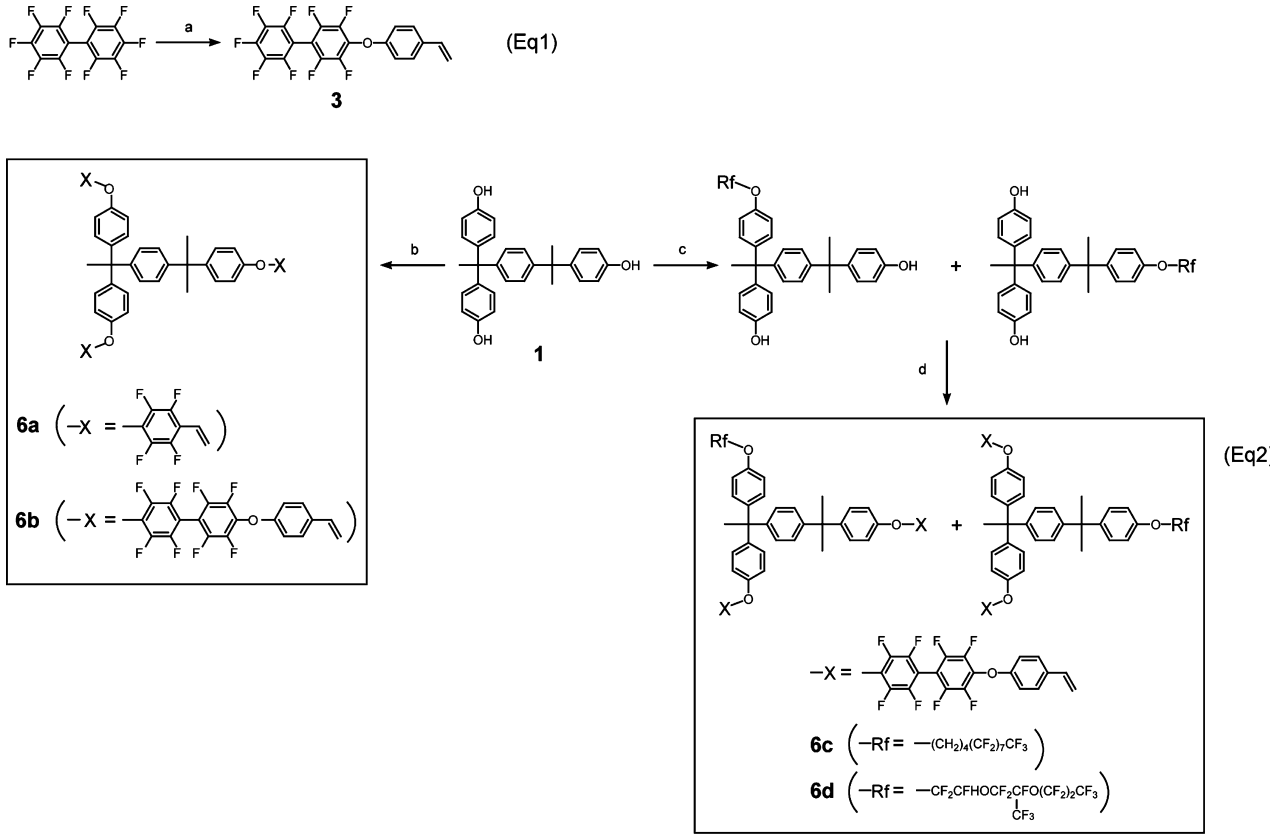

[a] Reagents and conditions: (a) 4-acetoxystyrene, KOH, water, THF, rt; (b) **2** or **3**, K_2CO_3, DMF, 70 °C; (c) **4** or **5**, K_2CO_3, DMF, 70 °C; (d) **3**, K_2CO_3, DMF, 70 °C.

it becomes possible to endow low-*k* materials with patterning capabilities. Selective cross-linking reactions occurring only on UV-irradiated regions generate patterned low-*k* insulator films, which can eliminate the need for sacrificial patterning materials and thereby greatly simplify device fabrication processes. Recently, a few groups have attempted to append patterning properties onto polymeric structures (18−21). In particular, Hasegawa and Tominaga suggested environmentally friendly photopatternable low-*k* polyimides, which still require the use of alcohols, glycols, or their monoalkyl ethers for pattern development (18).

Hydrofluoroethers (HFEs) are environmentally friendly fluorous solvents that have been introduced as replacements for chlorofluorocarbons and hydrochlorofluorocarbons (22). In addition to their environmental advantages, HFEs have another important benign characteristic in terms of materials processing. Because of their high fluorine content, HFEs do not interact heavily with nonfluorinated organic or polymeric materials. Recently, Zakhidov et al. reported that HFEs are chemically friendly to organic electronic materials (23, 24) and could enable the fabrication of multiple-layer organic devices by photolithographic techniques. From this context, it is expected that the processing of low-*k* materials in HFEs would provide a simpler and more environmentally responsible fabrication process as well as a new approach to building complicated organic electronic devices. This concept is further rationalized by the fact that highly fluorinated low-*k* materials can be easily processed in those highly fluorinated solvents.

Herein, we report a series of low-*k* materials based on small molecular precursors that have fluorinated substituents. The synthesis and evaluation of thermal and dielectric properties are also described. Finally, we demonstrate the photolithographic patterning of the molecular precursors in HFEs under UV-exposure conditions.

RESULTS AND DISCUSSION

Design and Synthesis of Low-*k* Precursor Materials. The synthetic procedures for the small molecular precursors are illustrated in Scheme 1. The design of the molecular structure was based on the following ideas: (i) a bulky aromatic core for thermal stability, low film density, and amorphous film-forming properties, (ii) styrenic end groups for cross-linking, (iii) fluorinated side chains for sufficient solubility in HFEs, thermal stability, and low polarizability. Furthermore, because fluorinated compounds are hydrophobic, we can also expect to prevent moisture uptake that compromises the device performance. For the core of these molecular materials, the commercially available compound α,α,α′-tris(4-hydroxyphenyl)-1-ethyl-4-isopropylbenzene (**1**) was employed. The low-*k* precursors **6a** and **6b** were synthesized via one-step nucleophilic aromatic substitution reactions under basic conditions between **1** and pentafluorostyrene (**2**) or 4-nonafluorobiphenyloxystyrene

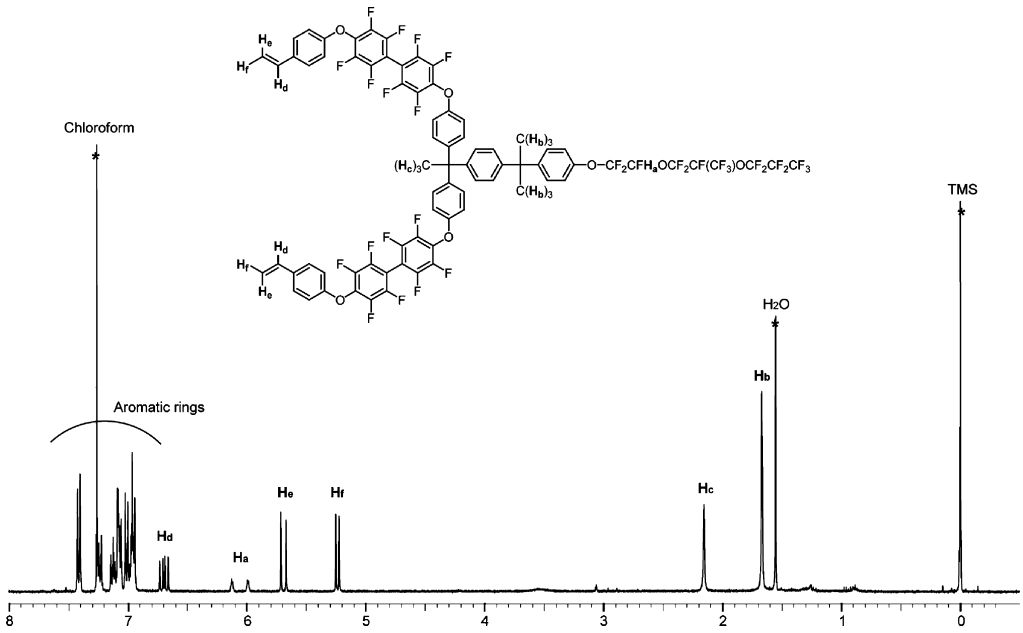

FIGURE 1. ^{1}H NMR spectrum of 6d.

(**3**), respectively. Nucleophilic attack by corresponding phenoxides occurred at the para positions of the fluorinated aromatic rings instead of the ortho or meta positions. The fluorostyrene **3** was prepared in advance by adding a potassium hydroxide (KOH) aqueous solution to a mixture of 4-acetoxystyrene and decafluorobiphenyl in tetrahydrofuran (THF; eq 1 in Scheme 1). Subsequent column chromatographic separation removed unreacted decafluorobiphenyl and the disubstituted compound to give the monosubstituted compound **3** in 31% yield. The precursors **6c** and **6d**, on the other hand, required a two-step synthesis; the first stage was a monosubstitution reaction of **1** with 1,1,1,2,2,3,3,4,4,5,5,6,6,7,7,8,8-heptadecafluoro-12-iododododecane (**4**) (25, 26) or perfluoro(5-methyl-3,6-dioxanon-1-ene) (**5**) in the presence of K_2CO_3 as a base. The reaction between **1** and **4** was a nucleophilic substitution reaction, while the reaction of **1** and **5** was an addition reaction (26, 27) of OH groups to the trifluorovinyl ether moiety in **5**. The monosubstituted compounds separated by column chromatography were then reacted with the fluorostyrene **3** to give the desired compounds **6c** and **6d** in high yields. These precursors **6c** and **6d** were theoretically a mixture of regioisomers as shown in Scheme 1, which favorably stabilize the amorphous nature of those low-*k* precursors, despite the fact that NMR and thin-layer chromatography did not indicate sufficient differences. All precursors **6a**−**6d** were characterized by ^{1}H and ^{19}F NMR, elemental analysis, and mass spectrometry. The ^{1}H NMR spectrum of the precursor **6d**, for example, is illustrated in Figure 1. Two singlet peaks of protons H_b and H_c of the two methyl groups were observed at 1.67 and 2.15 ppm, respectively. The characteristic doublet peak at 6.06 ppm with the coupling constant of 53 Hz was assigned to the proton H_a. The corresponding fluorine at the H_a carbon was observed at −145.5 ppm in ^{19}F NMR. These chemical shifts and the coupling constant of the $-OCFH_a-$ group were consistent with those of the previous report (27).

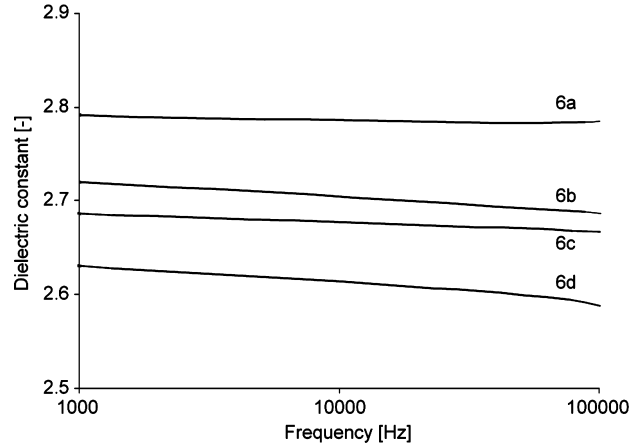

FIGURE 2. Dielectric constant curves.

Dielectric Properties. The dielectric constant of cross-linked films of the precursor **6a**−**6d** was directly determined by a capacitance measurement at various frequencies. The capacitors were fabricated on a gold-backed silicon wafer by spin-coating the precursor solutions, which contained 5 wt % *N*-nonafluorobutanesulfonyloxy-1,8-naphthalimide (**7**) (28) as a photoacid generator (PAG). After UV ($\lambda = 365$ nm) exposure with a dose of 3000 mJ cm^{-2}, the wafer was baked at 80 °C for 5 min to effect a cross-linking reaction. Finally aluminum and titanium were deposited (diameter = 10 mm) as a top electrode. The thickness of each cross-linked film was measured by ellipsometry. Figure 2 shows the measured *k* values of about 2.6−2.8 according to variation of the operating frequency. It should be noted that the dielectric constants exhibited by these cross-linked materials are significantly lower than that of silicon dioxide (3.9) and comparable to the values of polymeric low-*k* materials [e.g., polyimides (3.1−3.4) (1), SiLK (2.65) (6), or benzocyclobutene (BCB)-based polymer (2.65) (17)].

The cross-linked films of the precursors exhibited a clear trend in their dielectric constants; the *k* values gradually

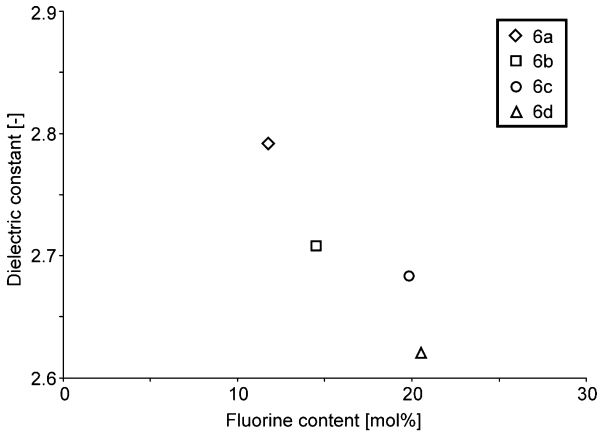

FIGURE 3. Relationship between the dielectric constant (at 10 kHz) and molar fluorine content.

decreased in accordance with the molar fluorine content (Figure 3). The interesting fact here was that the films of the precursors **6c** and **6d**, which had almost the same molar fluorine content (20% and 21%, respectively), showed a relatively large difference of *k* values. It is assumed that the perfluorinated side chain in **6d** can afford smaller polarizability against externally applied electric fields compared with the semiperfluorinated side chain in **6c**. Furthermore, the branched side-chain structure of **6d** likely allows for a larger free volume inside the film, which can also contribute to a lower *k* value.

The surface uniformity of the cross-linked film of precursor **6d**, as the best candidate, was also observed via atomic force microscopy (AFM) along with the films derived from precursors **6b** and **6c**. As shown in Figure 4, the roughness of the films was negligible (0.25−0.43 nm) and there was an absence of pinholes, both desirable properties for constructing robust insulators. Other factors of precursor **6d** including the refractive index (1.49 at 630 nm), dissipation factor, and capacitance were also measured (Figure 5). The low refractive index compared to other polymeric materials, e.g., SiLK (1.63 at 633 nm) (6), can be attributed to the incorporation of the fluorinated structure. The dissipation factor, which is also important to evaluate the device performance, was relatively low (0.003−0.02), enough to expect low power loss of the films.

Thermal Properties. The thermal properties of the precursors **6a**−**6d** were examined by differential scanning calorimetry (DSC) and thermogravimetric analysis (TGA) (Figure 6). The decomposition temperature at 10 wt % loss of each precursor was around 450 °C, which is sufficiently high for microelectronics fabrication processes (1). Usually, cross-linking of thermoset precursors improves the thermal stability. We thus can expect at least similar or even better thermal properties for the cross-linked materials. This outstanding thermal stability could be due to the aromatic core structure and the incorporation of fluorine atoms into the side chains. DSC analysis indicated that all of the precursors **6a**−**6d** did not show crystalline properties but had glass transition temperatures (T_g's) of 37, 61, 44, and 36 °C, respectively. This amorphous nature is essential to forming robust films for insulating layers.

The thermal properties of the cross-linked precursor films were also examined; DSC analysis of **6c** was carried out as an example. In Figure 7A, the first and second heating curves of the precursor **6c** alone and a mixture of **6c** with PAG **7** after UV exposure are shown. In the absence of PAG, the precursor **6c** appeared to vitrify after the first heat/cool cycle. On the other hand, the mixture with PAG no longer revealed a similar glass transition behavior after the first heating, and there was no glass transition temperature in the range of the DSC running up to 250 °C. This must be due to a cross-linking reaction during the first heating process. The exothermic response in the first heating process would also support this hypothesis. Despite the fact that the small molecular precursors exhibit relatively low T_g's, their cross-linked films are thermally robust enough for subsequent processing in low-*k* applications. Moreover, the DSC study provides evidence of the cross-linking reaction of the styrenic groups in **6a**−**6d** through acid generation from the PAG **7** under UV exposure conditions, as illustrated in Figure 7B, which enables the photolithographic patterning of the precursors.

Solubility in HFEs. The solubility of each precursor in HFE-7100, -7200, and -7500 (Figure 8) was examined to identify the best developer during lithographic patterning; films were immersed in each solvent and overtime changes in the film thickness were measured by profilometry. HFE-7100 proved best in terms of developing **6c** or **6d**, whereas **6a** and **6b** did not dissolve well in any HFE solvents. The better solubility of **6c** and **6d** can be attributed to their higher molar fluorine content. Figure 9 shows the film thickness changes for the precursors **6b**−**6d** in HFE-7100. As expected, **6d** dissolves much faster than **6c** in spite of their similar molar fluorine contents; the dissolution rates of **6c** and **6d** calculated from the decrease of the film thickness at 120 s were 2 and 3 nm s^{-1}, respectively. It is postulated that the good affinity between HFEs and the perfluorinated alkyl ether substituent of **6d** is responsible for this solubility difference. Thus, the precursor **6d** and HFE-7100 were chosen to demonstrate photolithographic patterning.

Evaluation of Photolithographic Patterning in HFEs. To evaluate the photolithographic patterning performance, spin-coated films of the precursor **6d** with PAG **7** (5 wt % with respect to **6d**) were prepared. The uniform films were exposed by UV light (λ = 365 nm) through a photomask under different conditions (doses ranging from 500 to 1700 mJ cm^{-2}), and films were baked at 50, 60, 70, or 80 °C for 5 min. The exposed films were developed in HFE-7100 to give fine negative-tone images. The mildest conditions that we found to obtain fine patterns were an exposure dose of 1000 mJ cm^{-2} and a postexposure bake (PEB) at 50 °C for 5 min. Figure 10 displays optical images patterned at this dose and PEB conditions, confirming that even high-resolution submicrometer features can be achieved successfully. Photoimageable low-*k* materials reported thus far demand the use of aggressive developers; however, precursor **6d** can be processed in chemically benign and environmentally friendly solvents. Furthermore, the compatibility

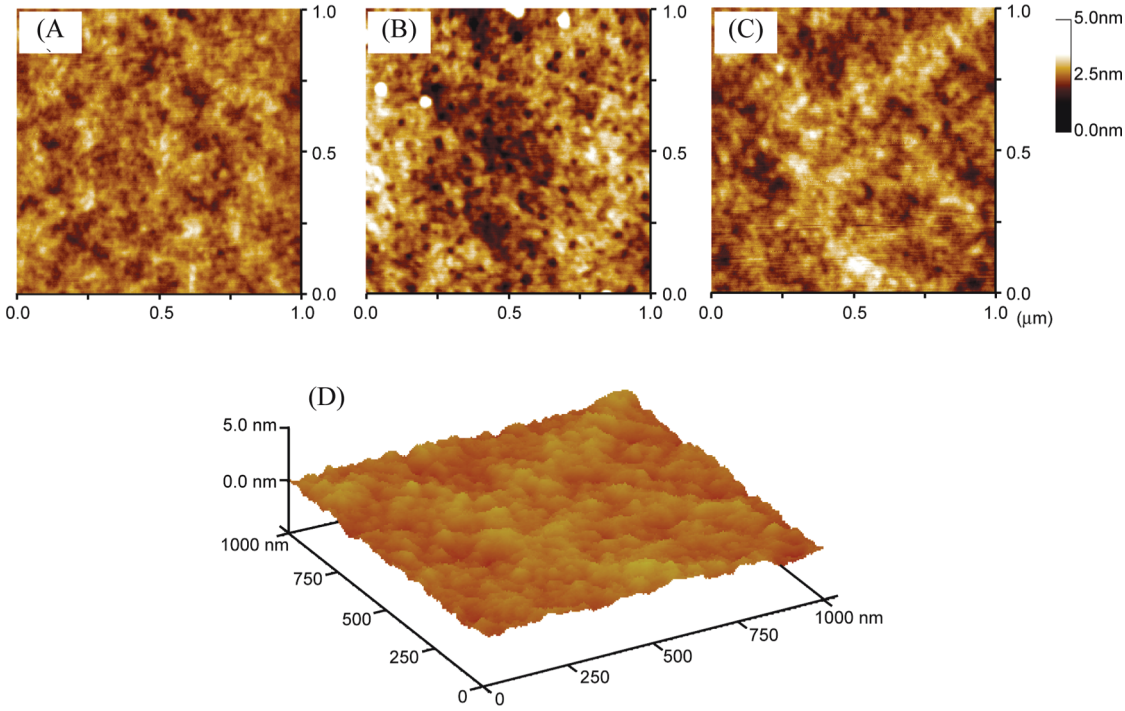

FIGURE 4. AFM height images: (A) 6b top; (B) 6c top; (C) 6d top; (D) 6d diagonal view.

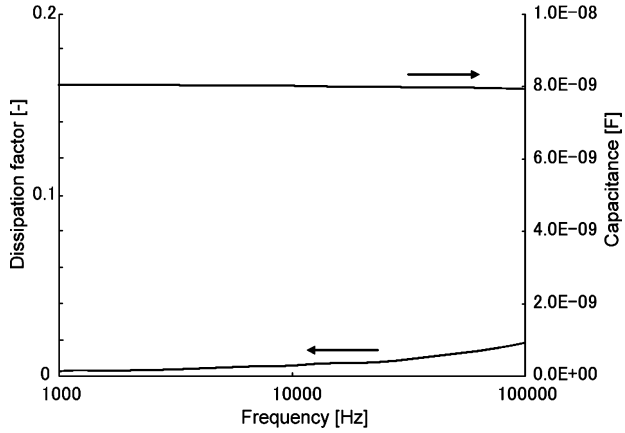

FIGURE 5. Dissipation and capacitance curves of the cross-linked 6d films.

of HFE solvents with common organic or polymeric materials makes the incorporation of these low-*k* compounds into more complicated multiple-layer device structures possible.

CONCLUSIONS

We have demonstrated the synthesis, characterization, and patterning properties of a series of low-*k* materials achieved by cross-linking small molecular precursors. The precursors **6a**−**6d** showed high thermal stability up to 400 °C and exhibited an amorphous character essential to forming good-quality films. DSC analysis of the precursor **6c** mixed with PAG **7** ensured that the material cross-linked through UV exposure to afford a thermally robust film. AFM measurements showed a pinhole-free, very smooth surface of the cross-linked films, which is a promising property for device fabrication. Dielectric constants determined by capacitance measurements were 2.6−2.8 at 100 kHz, which are comparable to those of other conventional low-*k* polymers reported thus far. Photolithographic patterning of the precursor **6d** was also performed in HFE-7100 to give high-resolution negative-tone images on a submicrometer scale. This is the first report of solution-processable low-*k* materials and their patterning performance in environmentally friendly and chemically benign solvents.

EXPERIMENTAL SECTION

Materials. α,α,α′-Tris(4-hydroxyphenyl)-1-ethyl-4-isopropylbenzene (**1**) was purchased from TCI America. 4-Acetoxystyrene was obtained from Sigma-Aldrich. Pentafluorostyrene (**2**), decafluorobiphenyl, and perfluoro(5-methyl-3,6-dioxanon-1-ene) (**5**) were purchased from Oakwood Products, Matrix Scientific, and Synquest, respectively. All of these chemicals were used as received. 1,1,1,2,2,3,3,4,4,5,5,6,6,7,7,8,8-Heptadecafluoro-12-iodododecane (**4**) and *N*-nonafluorobutanesulfonyloxy-1,8-naphthalimide (**7**) were synthesized according to the literature (25, 28). Propylene glycol monomethyl ether acetate (PGMEA), benzotrifluoride, anhydrous tetrahydrofuran (THF), and anhydrous dimethylformamide (DMF) were purchased and used without further drying. 3M Novec Engineered Fluid HFE-7100, -7200, and -7500 were donated from 3M USA.

Characterization. ^{1}H and ^{19}F NMR spectra were recorded on a Varian Inova-400 (400 and 376 MHz, respectively) spectrometer at ambient temperature. All chemical shifts are quoted in parts per million (ppm) relative to the internal reference, and coupling constants *J* are measured in hertz. The multiplicity of the signal is indicated as follows: s (singlet), d (doublet), t (triplet), q (quartet), m (multiplet), dd (doublet of doublets), dt (doublet of triplets), dm (doublet of multiplets), and br s (broad singlet). Microanalyses were carried out by Quantitative Technologies, Inc. Mass spectrometry was performed by the Department of Molecular Biology and Genetics, Cornell University, Ithaca, NY. TGA was performed on a TA Instruments Q500 at a heating rate of 10 °C min^{-1} under N_2. The glass transition temperature (T_g) was measured on a TA Instruments Q1000 modulated differential scanning calorimeter (DSC) at a heat/cool rate of 10 °C min^{-1} under N_2 for heat/cool/heat cycles. The dielectric constant was measured on a broad-band dielectric

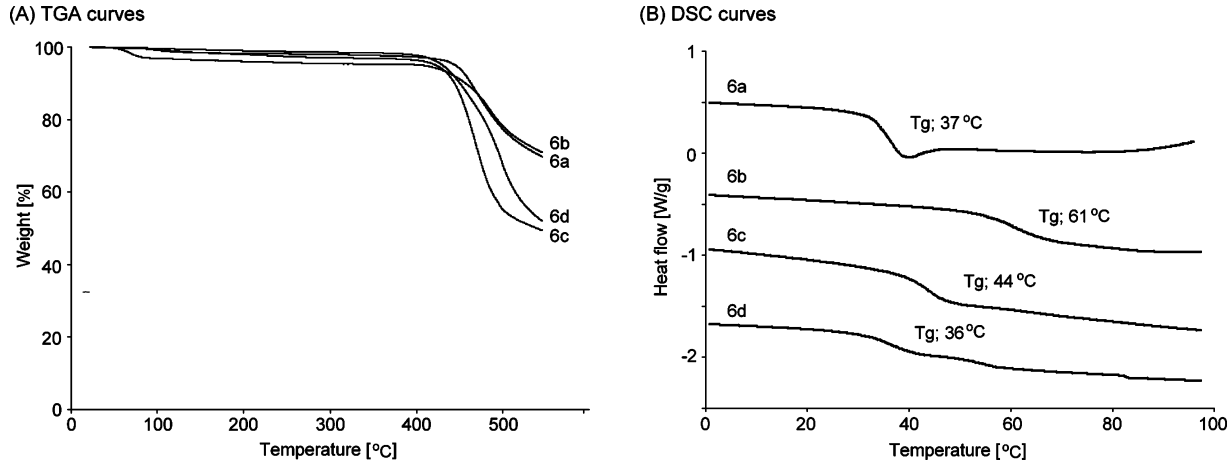

FIGURE 6. (A) TGA and (B) DSC curves of the precursors.

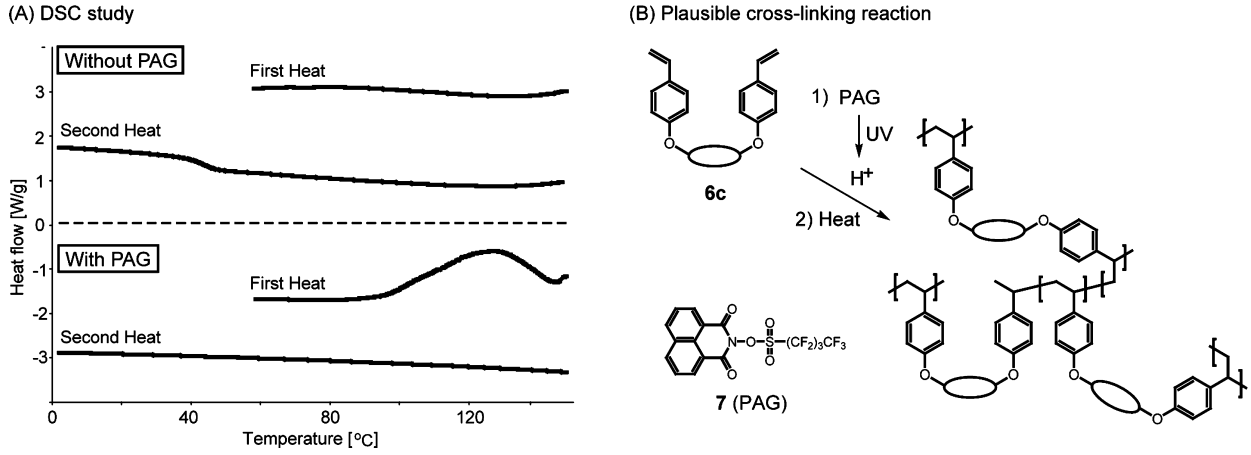

FIGURE 7. (A) DSC study of 6c with and without PAG after UV exposure. (B) Possible cross-linking reaction in the presence of PAG.

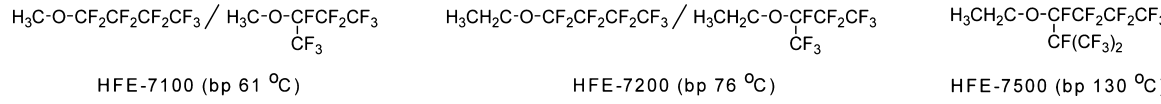

FIGURE 8. HFEs used in this study.

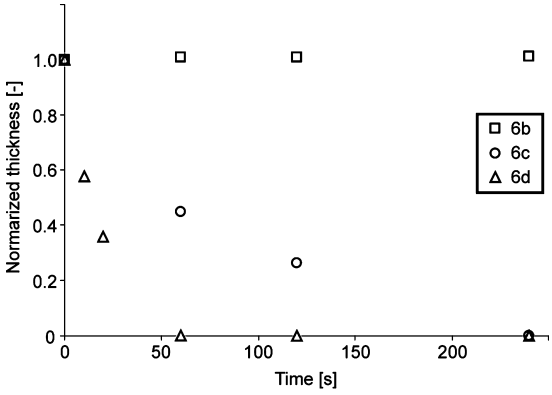

FIGURE 9. Solubility behavior in HFE-7100.

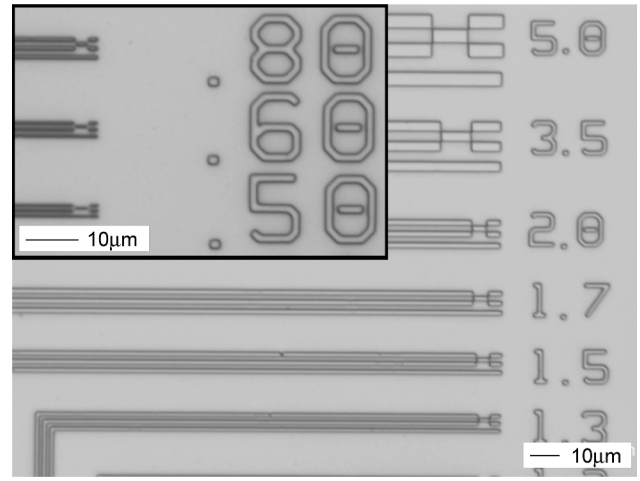

FIGURE 10. Optical images of 6d developed in HFE-7100. Numbers drawn at the right side of the patterns are feature sizes (μm) of the lines and spaces.

spectrometer, Novocontrol Turnkey Concept N40, at ambient temperature. AFM was performed on a Veeco Dimension 3100. Ellipsometry was performed on a Woollam M-2000, and profilometry was carried out by using a Tencor P-10 surface profiler.

Synthesis of Fluorinated Styrenic Compound 3. To a 50 cm^3 round-bottomed flask were added decafluorobiphenyl (9.98 g, 29.8 mmol), 4-acetoxystyrene (4.31 g, 26.6 mmol), and THF (10 cm^3). The mixture was stirred in an ice/water bath, and then a 43 wt % potassium hydroxide (KOH) aqueous solution (7.30 g) was added dropwise. After it was

warmed to ambient temperature, the solution was stirred for 24 h. The solution was diluted in Et_2O and washed with brine three times. The separated organic layer was dried over anhydrous $MgSO_4$ and concentrated under reduced pressure to give a crude product as a pale-yellow solid. The solid was dissolved in acetone again and then purified through flash column chromatography (silica gel, hexanes). Unreacted decafluorobiphenyl (1.55 g) was recovered, and the desired styrene **3** was obtained as a white solid (3.35 g, 31% yield from 4-acetoxystyrene). ^{1}H NMR (400 MHz, $CDCl_3$): δ 5.23 (dd, J = 0.6 and 11.1 Hz, 1H, $-$PhCH=CH_2), 5.69 (dd, J = 0.6 and 17.4 Hz, 1H, $-$PhCH=CH_2), 6.69 (dd, J = 11.1 and 17.7 Hz, 1H, $-$PhCH=CH$_2$), 7.01 (d, J = 8.4 Hz, 2H, $-$*Ph*CH=CH$_2$), 7.41 (d, J = 8.7 Hz, 2H, $-$*Ph*CH=CH$_2$). ^{19}F NMR (376 MHz, $CDCl_3$): δ $-$137.9 (2F), $-$138.7 (2F), $-$150.7 (1F), $-$153.4 (2F), $-$161.1 (2F). Elem anal. Calcd for $C_{20}H_7F_9O$: C, 55.3; H, 1.6. Found: C, 55.3; H, 1.6.

Synthesis of Trifunctional Precursor 6a. To a 50 cm^3 round-bottomed flask were added **1** (1.00 g, 2.35 mmol), **2** (1.52 g, 7.83 mmol), and anhydrous DMF (10 cm^3). The solution was stirred at 60 °C, and then K_2CO_3 powder (1.00 g, 14.5 mmol) was added into the solution. After stirring for 16 h, additional **2** (0.50 g, 2.57 mmol) was added and kept stirring for 5 h. The solution was poured into Et_2O and then washed with brine three times. The separated organic layer was dried over anhydrous $MgSO_4$ and concentrated under reduced pressure to give a white solid. Through flash column chromatography (silica gel, 1/1 hexanes/benzotrifluoride), the crude product was purified and a white glassy solid **6a** was obtained (2.07 g, 93%). ^{1}H NMR (300 MHz, $CDCl_3$): δ 1.64 (s, 6H, Me), 2.12 (s, 3H, Me), 5.71 (d, J = 12.0 Hz, 3H, $-$CH=CH_2), 6.10 (d, J = 18.0 Hz, 3H, $-$CH=CH_2), 6.67 (dd, J = 11.7 and 18.0 Hz, 3H, $-$CH=CH$_2$), 6.84$-$7.19 (m, 16H, aromatic). ^{19}F NMR (282 MHz, $CDCl_3$): δ $-$144.3 (6F), $-$155.8 (6F). Elem anal. Calcd for $C_{53}H_{34}F_{12}O_3$: C, 67.2; H, 3.6. Found: C, 67.0; H, 3.4.

Synthesis of Trifunctional Precursor 6b. The synthesis followed the same procedure as for that for precursor **6a**. **1** (0.51 g, 1.19 mmol), **3** (1.59 g, 3.66 mmol), K_2CO_3 powder (0.89 g, 6.45 mmol), and anhydrous DMF (10 cm^3) were used. Through flash column chromatography (silica gel, 4/1 hexanes/benzotrifluoride and then 1/1 hexanes/Et_2O), the crude product was purified to give a white fluffy solid **6b** (2.09 g, 99%). ^{1}H NMR (400 MHz, $CDCl_3$): δ 1.67 (s, 6H, Me), 2.16 (s, 3H, Me), 5.23 (d, J = 11.1 Hz, 3H, $-$PhCH=CH_2), 5.69 (d, J = 17.4 Hz, 3H, $-$PhCH=CH_2), 6.70 (dd, J = 10.8 and 17.4 Hz, 3H, $-$PhCH=CH$_2$), 6.94$-$7.25 (m, 22H, aromatic), 7.41 (d, J = 8.7 Hz, 6H, aromatic). ^{19}F NMR (376 MHz, $CDCl_3$): δ $-$138.7 (12F), $-$153.6 (12F). Elem anal. Calcd for $C_{89}H_{46}F_{24}O_6$: C, 64.1; H, 2.8. Found: C, 63.7; H, 2.6. ESI: *m/z* 1668.46 (M + H)$^+$. Calcd for $C_{89}H_{47}F_{24}O_6$: *m/z* 1668.28.

Synthesis of Bifunctional Precursor 6c. To a magnetically stirred solution of **4** (1.13 g, 1.88 mmol) and **1** (1.03 g, 2.43 mmol) in anhydrous DMF (10 cm^3) was added K_2CO_3 powder (0.48 g, 3.48 mmol) at 70 °C. After stirring for 24 h, the solid was removed by filtration, and then a 1 N HCl aqueous solution was added to the filtrate. Additionally, EtOAc was added, and the diluted solution was washed with brine three times. The extracted organic layer was dried over anhydrous $MgSO_4$ and concentrated under reduced pressure to give an orange viscous liquid. The liquid was dissolved in a mixture of hexanes and EtOAc (4/1 by volume) and then purified by flash column chromatography (silica gel, 4/1 hexanes/EtOAc and then 3/1). The monosubstituted compound (0.88 g, 52% from **4**) and disubstituted compound (0.49 g, 19% from **4**) were obtained. Unreacted **1** was also recovered (0.55 g). The obtained monosubstituted compound (0.60 g, 0.67 mmol) and **3** (0.80 g, 1.84 mmol) were dissolved in anhydrous DMF. To the solution was added K_2CO_3 (0.63 g, 4.56 mmol) at 70 °C. After vigorous stirring for 20 h, the solution was diluted with benzotrifluoride and then washed with brine three times. The separated organic layer was dried over anhydrous $MgSO_4$ and concentrated under reduced pressure to give a white solid. The crude product was purified by flash column chromatography (silica gel, hexanes only, and then 95/5 hexanes/EtOAc) to give the white glassy solid **6c** (1.08 g, 94% from the monosubstituted compound). ^{1}H NMR (400 MHz, $CDCl_3$): δ 1.67 (s, 6H, Me), 1.84 (m, 4H, $-CH_2-$), 2.13$-$2.16 (m, 5H, Me and $-CH_2CF_2-$), 3.98 (m, 2H, $-OCH_2-$), 5.24 (d, J = 10.8 Hz, 2H, $-$PhCH=CH_2), 5.69 (d, J = 17.6 Hz, 2H, $-$PhCH=CH_2), 6.70 (dd, J = 10.8, 17.6 Hz, 2H, $-$PhCH=CH$_2$), 6.92$-$7.25 (m, 20H, aromatic), 7.41 (d, J = 8.4 Hz, 4H, aromatic). ^{19}F NMR (376 MHz, $CDCl_3$): δ $-$80.0 (3F), $-$113.8 (2F), $-$121.3 (6F), $-$122.1 (2F), $-$122.9 (2F), $-$125.5 (2F), $-$137.4 (8F), $-$152.3 (8F). Elem anal. Calcd for $C_{81}H_{47}F_{33}O_5$: C, 56.3; H, 2.7. Found: C, 56.0; H, 2.6. ESI: *m/z* 1728.53 (M + H)$^+$. Calcd for $C_{81}H_{48}F_{33}O_5$: *m/z* 1728.18.

Synthesis of Bifunctional Precursor 6d. The synthesis followed the same procedure as that for precursor **6c**. **5** (1.14 g, 2.64 mmol), **1** (1.02 g, 2.40 mmol), K_2CO_3 powder (0.33 g, 2.39 mmol), and anhydrous DMF (10 cm^3) were prepared. The monosubstituted compound (0.64 g, 28% from **5**) and a mixture of disubstituted and trisubstituted compounds (0.96 g) were separated by flash column chromatography (silica gel, 3/1 hexanes/EtOAc and then 2/1). The obtained monosubstituted compound (0.32 g, 0.37 mmol), **3** (0.36 g, 0.82 mmol), and K_2CO_3 (0.35 g, 2.53 mmol) were mixed in anhydrous DMF. The crude product was purified by flash column chromatography (silica gel, 30/1 hexanes/EtOAc and then 95/5) to give the white glassy solid **6d** (0.59 g, 94% from the monosubstituted compound). ^{1}H NMR (400 MHz, $CDCl_3$): δ 1.67 (s, 6H, Me), 2.15 (s, 3H, Me), 5.24 (d, J = 11.2 Hz, 2H, $-$PhCH=CH_2), 5.69 (d, J = 17.6 Hz, 2H, $-$PhCH=CH_2), 6.06 (d, J = 53.2 Hz, 1H, $-$CF$H-$), 6.70 (dd, J = 10.8 and 17.6 Hz, 2H, $-$PhCH=CH$_2$), 6.94$-$7.25 (m, 20H, aromatic), 7.41 (d, J = 8.4 Hz, 4H, aromatic). ^{19}F NMR (376 MHz, $CDCl_3$): δ $-$80.4 (3F), $-$81.6 (3F), $-$82.2 to $-$86.8 (6F), $-$130.1 (2F), $-$138.5 (8F), $-$145.1 (1F), $-$145.7 (1F), $-$153.5 (8F). Elem anal. Calcd for $C_{77}H_{40}F_{32}O_7$: C, 54.9; H, 2.4. Found: C, 55.3; H, 2.3. ESI: *m/z* 1686.40 (M + H)$^+$. Calcd for $C_{77}H_{41}F_{32}O_7$: *m/z* 1686.09.

Photolithographic Patterning. The lithographic patterning of the precursor **6d** on a silicon substrate was performed by using a GCA Autostep 200 DSW i-line Wafer Stepper. The films were spin-coated from a 8 wt % solution of compound **6d** (0.20 g) in a mixed solvent of benzotrifluoride (2.0 g) and PGMEA (0.4 g) containing 5% PAG **7** (w/w, with respect to **6d**). The spin coating was carried out at 1500 rpm (acceleration: 400 rpm s^{-1}) for 40 s, followed by a post apply bake at 70 °C for 60 s. The resulting film had a thickness of ca. 360 nm. The adequate exposure dose was 1000 mJ cm^{-2}. After exposure, the film was baked (PEB) at 50 °C for 5 min and then developed in HFE-7100 at ambient temperature for 60 s.

Acknowledgment. This research was accomplished with the financial support of Asahi Glass Co., Ltd. J.-K.L. thanks the National Science Foundation (Materials World Network DMR-0602821). M.C. and A.A.Z. thank the New York State Foundation for Science, Technology and Innovation (NYSTAR). We also thank the Cornell Nanoscale Facility, Nanobiotechnology Center, and Cornell Center for Materials Research for the use of their equipment.

REFERENCES AND NOTES

(1) Maier, G. *Prog. Polym. Sci.* **2001**, *26*, 3–65.
(2) Bucholz, T. L.; Li, S. P.; Loo, Y. L. *J. Mater. Chem.* **2008**, *18*, 530–536.
(3) Cha, B. J.; Yang, J. M. *J. Appl. Polym. Sci.* **2007**, *104*, 2906–2912.
(4) Fu, G. D.; Yuan, Z. L.; Kang, E. T.; Neoh, K. G.; Lai, D. M.; Huan, A. C. H. *Adv. Funct. Mater.* **2005**, *15*, 315–322.

(5) Long, T. M.; Swager, T. M. *J. Am. Chem. Soc.* **2003**, *125*, 14113–14119.
(6) Martin, S. J.; Godschalx, J. P.; Mills, M. E.; Shaffer, E. O.; Townsend, P. H. *Adv. Mater.* **2000**, *12*, 1769–1778.
(7) Nunoshige, J.; Akahoshi, H.; Shibasaki, Y.; Ueda, M. *Chem. Lett.* **2007**, *36*, 238–239.
(8) Tsuchiya, K.; Shibasaki, Y.; Aoyagi, M.; Ueda, M. *Macromolecules* **2006**, *39*, 3964–3966.
(9) Xi, K.; Guo, R.; Weng, Y. Y.; He, H.; Shao, Q.; Cai, J.; Chen, Q. M.; Yu, X. H.; Jia, X. D. *J. Appl. Polym. Sci.* **2007**, *103*, 1238–1243.
(10) Lemal, D. M. *J. Org. Chem.* **2004**, *69*, 1–11.
(11) Ding, S. J.; Wang, P. F.; Zhang, D. W.; Wang, J. T.; Lee, W. W. *Mater. Lett.* **2001**, *49*, 154–159.
(12) Goto, K.; Akiike, T.; Inoue, Y.; Matsubara, M. *Macromol. Symp.* **2003**, *199*, 321–331.
(13) Buckley, L. J.; Snow, A. W.; Hu, H. S.; Griffith, J.; Ray, M. *J. Vac. Sci. Technol. B* **1997**, *15*, 741–745.
(14) Hu, H. S. W.; Griffith, J. R.; Buckley, L. J.; Snow, A. W. *ACS Symp. Ser.* **1995**, *614*, 369–378.
(15) Hu, H. S. W.; Griffith, J. R. *ACS Symp. Ser.* **1994**, *537*, 507–516.
(16) Liu, J. G.; Shang, Y. M.; Fan, L.; Yang, S. Y. *Acta Polym. Sin.* **2003**, 565–570.
(17) Mills, M. E.; Townsend, P.; Castillo, D.; Martin, S.; Achen, A. *Microelectron. Eng.* **1997**, *33*, 327–334.
(18) Hasegawa, M.; Tominaga, A. *J. Photopolym. Sci. Technol.* **2005**, *18*, 307–312.
(19) Qian, Z. G.; Ge, Z. Y.; Li, Z. X.; He, M. H.; Liu, J. G.; Pang, Z. Z.; Fan, L.; Yang, S. Y. *Polymer* **2002**, *43*, 6057–6063.
(20) Shi, F. F.; Schneggenburger, L. A.; Economy, J. *J. Appl. Polym. Sci.* **1997**, *63*, 1199–1211.
(21) Lyu, Y. Y.; Yim, J. H.; Byun, Y.; Kim, J. M.; Jeon, J. K. *Thin Solid Films* **2006**, *496*, 526–532.
(22) Tsai, W. T. *J. Hazard. Mater.* **2005**, *119*, 69–78.
(23) Zakhidov, A. A.; Lee, J. K.; Fong, H. H.; DeFranco, J. A.; Chatzichristidi, M.; Taylor, P. G.; Ober, C. K.; Malliaras, G. G. *Adv. Mater.* **2008**, *20*, 3481–3484.
(24) Lee, J.-K.; Chatzichristidi, M.; Zakhidov, A. A.; Taylor, P. G.; DeFranco, J. A.; Hwang, H. S.; Fong, H. H.; Holmes, A. B.; Malliaras, G. G.; Ober, C. K. *J. Am. Chem. Soc.* **2008**, *130*, 11564–11565.
(25) Alvey, L. J.; Meier, R.; Soos, T.; Bernatis, P.; Gladysz, J. A. *Eur. J. Inorg. Chem.* **2000**, *197*, 5–1983.
(26) Furin, G. G.; Pressman, L. S.; Pokrovsky, L. M.; Krysin, A. P.; Chi, K. W. *J. Fluorine Chem.* **2000**, *106*, 13–24.
(27) Dlouha, I.; Kvicala, J.; Paleta, O. *J. Fluorine Chem.* **2002**, *117*, 149–159.
(28) Iwashima, C.; Imai, G.; Okamura, H.; Tsunooka, M.; Shirai, M. *J. Photopolym. Sci. Technol.* **2003**, *16*, 91–96.

AM9004978